

Cooling of neutron stars with diffusive envelopes

M. V. Beznogov^{1*}, M. Fortin², P. Haensel², D. G. Yakovlev³, J. L. Zdunik²

¹*St Petersburg Academic University, 8/3 Khlopina st., St Petersburg 194021, Russia*

²*Nicolaus Copernicus Astronomical Center, Bartycka 18, Warsaw 00-716, Poland*

³*Ioffe Institute, 26 Politekhnicheskaya st., St Petersburg 194021, Russia*

Accepted . Received ; in original form

ABSTRACT

We study the effects of heat blanketing envelopes of neutron stars on their cooling. To this aim, we perform cooling simulations using newly constructed models of the envelopes composed of binary ion mixtures (H–He, He–C, C–Fe) varying the mass of lighter ions (H, He or C) in the envelope. The results are compared with those calculated using the standard models of the envelopes which contain the layers of lighter (accreted) elements (H, He and C) on top of the Fe layer, varying the mass of accreted elements. The main effect is that the chemical composition of the envelopes influences their thermal conductivity and, hence, thermal insulation of the star. For illustration, we apply these results to estimate the internal temperature of the Vela pulsar and to study the cooling of neutron stars of ages of $10^5 - 10^6$ yr at the photon cooling stage. The uncertainties of the cooling models associated with our poor knowledge of chemical composition of the heat insulating envelopes strongly complicate theoretical reconstruction of the internal structure of cooling neutron stars from observations of their thermal surface emission.

Key words: dense matter – plasmas – diffusion – stars: neutron – stars: evolution

1 INTRODUCTION

The long-standing problem of modern studies of neutron stars is to investigate the properties of superdense matter in their cores. One of a few methods to achieve this goal is to study the thermal evolution of neutron stars (particularly, cooling of isolated stars) and compare the theoretical models with the available observational data (e.g., Yakovlev & Pethick 2004; Page et al. 2009; Potekhin, Pons & Page 2015 and references therein). Different models of superdense matter predict different rates of neutrino cooling of neutron star interiors and, therefore, different surface temperatures as they are directly related to the internal temperatures. This allows one to select most suitable models of superdense matter from observations. It is a challenging task for many reasons, but we mainly focus on one of them. In order to explore the properties of superdense matter one needs to calculate (constrain) the internal temperature of the star from observations of its thermal surface emission.

We will restrict ourselves to not too young neutron stars (of age $t \gtrsim 10 - 100$ yr) which are thermally equilibrated and isothermal inside. The initial internal equilibration mainly consists in the equilibration between the crust

and the core of a star due to distinctly different microphysics there (e.g., Lattimer et al. 1994; Yakovlev et al. 2001 and references therein). After the equilibration the main temperature gradient in these stars still persists in a thin outer heat blanketing envelope with rather poor thermal conduction. It is usually sufficient to assume that this envelope extends from the atmosphere bottom to the layer of the density $\rho_b \sim 10^{10}$ g cm⁻³. Its thickness does not exceed a few hundred meters, and its mass is $\lesssim 10^{-8} - 10^{-7} M_\odot$. On the other hand, its mass cannot be smaller than the mass of the neutron star atmosphere (typically $\sim 10^{-18} - 10^{-16} M_\odot$). Let T_b be the temperature at the bottom density $\rho = \rho_b$. Although strong magnetic fields in the envelopes of neutron stars can affect the insulating properties of the envelopes and create an anisotropic distribution of the effective surface temperature T_s (e.g. Potekhin et al. 2003, 2015), we neglect such effects in the present paper. Our results cannot be used to study the thermal structure and evolution of neutron stars with very strong fields, particularly, magnetars. Even in this case the relation between T_s and T_b , required for cooling simulations and data analysis, is uncertain, mainly because of uncertain thermal conduction in the blanketing envelopes due to their unknown chemical composition.

Although the chemical composition of the heat blanketing envelopes is really uncertain, there are some natural limitations (see, e.g., Potekhin et al. 1997 and references

* E-mail: mikavb89@gmail.com

therein). For instance, at high temperatures T and/or densities ρ hydrogen transforms into helium due to thermo- or pycno-nuclear reactions and beta captures. Approximately, this happens at $T \gtrsim 4 \times 10^7$ K and/or $\rho \gtrsim 10^7$ g cm $^{-3}$. At higher $T \gtrsim 10^8$ K and/or $\rho \gtrsim 10^9$ g cm $^{-3}$, helium, in its turn, transforms into carbon. At still higher $T \gtrsim 10^9$ K and/or $\rho \gtrsim 10^{10}$ g cm $^{-3}$ carbon transforms into heavier elements.

The standard model of heat blanketing envelopes is the model developed by Potekhin, Chabrier & Yakovlev (1997) and elaborated by Potekhin et al. (2003). In this model (hereafter, the PCY97 model), the envelope is onion-like, composed of shells of pure elements with abrupt boundaries between the shells. The number of the shells is determined by a single parameter, ΔM , the accumulated mass of light elements (H, He, C). The width of each shell is limited by nuclear transformations of light elements. In the absence of light elements, the envelope is purely iron. In the presence of a thick layer of light elements, the envelope consists of consecutive shells of hydrogen, helium, carbon and iron. Although this model has proved to be useful, it relies on the assumption of abrupt boundaries between the layers of different chemical species and employs a specific dependence of the composition on the accumulated mass (governed by nuclear reactions and beta-captures).

Recently we have developed new models of diffusive heat blanketing envelopes (Beznogov, Potekhin & Yakovlev 2016) which consist of binary ion mixtures (either H–He, or He–C, or C–Fe) with a variable mass ΔM of light elements (either H, or He or C, respectively). They can be diffusively equilibrated or not. Since the ions have a tendency for separation, such an envelope consists of a top layer of lighter ions, a bottom layer of heavier ions, and a transition layer in between. While considering the equilibrated envelopes we have used proper relations for the ion diffusive currents taking into account the Coulomb coupling of the ions and the presence of temperature gradients. Note that Beznogov et al. (2016) have also introduced a characteristic transition density ρ^* from a lighter element to a heavier one instead of the mass of light elements ΔM . There is a one to one correspondence between ΔM and ρ^* .

Let us stress that according to Beznogov et al. (2016) the separation between the H and He ions, as well as between the C and Fe ones is rather strong (due to the gravitational force) leading to a narrow separation layer. In contrast, the separation between the He and C ions (which have almost the same charge-to-mass ratios) is slower (due to the Coulomb force), resulting in a wider transition layer. In any case, even at not very small deviations from diffusive equilibrium, the $T_s - T_b$ relation is rather insensitive to the structure of the transition zone and depends almost solely on ΔM . The $T_s - T_b$ relations have been calculated assuming different values of $\rho_b = 10^8, 10^9$ and 10^{10} g cm $^{-3}$ (which are suitable for different cooling problems; see Beznogov et al. 2016). For convenience of using in the computer codes, numerical results have been approximated by analytic expressions. To visualize the properties of the new heat blanketing envelopes, Beznogov et al. (2016) plotted (their figs. 1–7) representative profiles of particle fractions and temperatures in the envelopes as the functions of the density as well as the appropriate $T_s - T_b$ and $T_b - \Delta M$ relations. Note that those figures corresponded to a neutron star model with

mass $M = 1.4 M_\odot$ and radius $R = 10$ km; the same model will be used to interpret the observations of the Vela pulsar in Section 3.

Here we apply new envelope models to simulate cooling of the isolated middle-aged ($t \sim 10^2 - 10^6$ yr) neutron stars. We will use the PCY97 model as a reference for comparison. In Section 2 we present some formation scenarios of accreted envelopes. In Sections 3–5 we outline some calculations of internal structure and cooling of neutron stars with new envelope models. Our conclusions are formulated in Section 6.

2 FORMATION SCENARIOS

The composition of heat blanketing envelopes of neutron stars is uncertain. It can greatly vary depending on the formation history of the star and its evolutionary scenario.

Initially, it was thought that the envelopes (as well as neutron star atmospheres) contain heavy elements like iron, as a result of the formation of the envelope in a hot and very young star where light elements burnt-out into heavier ones. However, a more detailed analysis of the observed spectra of the thermal radiation originating from the atmospheres of neutron stars has shown that some spectra are better described by blackbody models (of iron atmosphere models) while others are better approximated by hydrogen atmosphere models (see, e.g., Potekhin 2014 and references therein). Moreover, the spectrum of the neutron star in the Cas A supernova remnant is well described by a carbon atmosphere model (Ho & Heinke 2009). The same is true for the neutron star in the supernova remnant HESS J1731–347 (Klochkov et al. 2013).

Therefore, the surface composition of thermally emitting neutron stars can be different. Naturally, the composition of the underlying envelopes can also be different. The composition of the surface layers can be affected by the fallback of material on the neutron star surface after the supernova explosion, by the accretion of hydrogen and helium from interstellar medium or from a binary companion (if the neutron star is or was in a compact binary), by the ion diffusion and the nuclear evolution in the neutron star envelope, and by other effects. A neutron star can directly accrete hydrogen and helium (e.g., Blaes et al. 1992). Alternatively, helium can be produced in nuclear reactions after the accretion of hydrogen. Helium can also burn further into carbon (see, e.g., Rosen 1968; Chang et al. 2010). In some cases the reverse process of spallation of heavier elements into lighter ones is possible. There are also indications that some transiently accreting neutron stars in low mass X-ray binaries in quiescent states have their outer envelopes composed of H and He which are left after an active accretion phase (Brown et al. 2002).

All in all, the composition of neutron star envelopes is largely unknown. It seems instructive to consider different models of the envelopes and to analyse observational manifestations of such models.

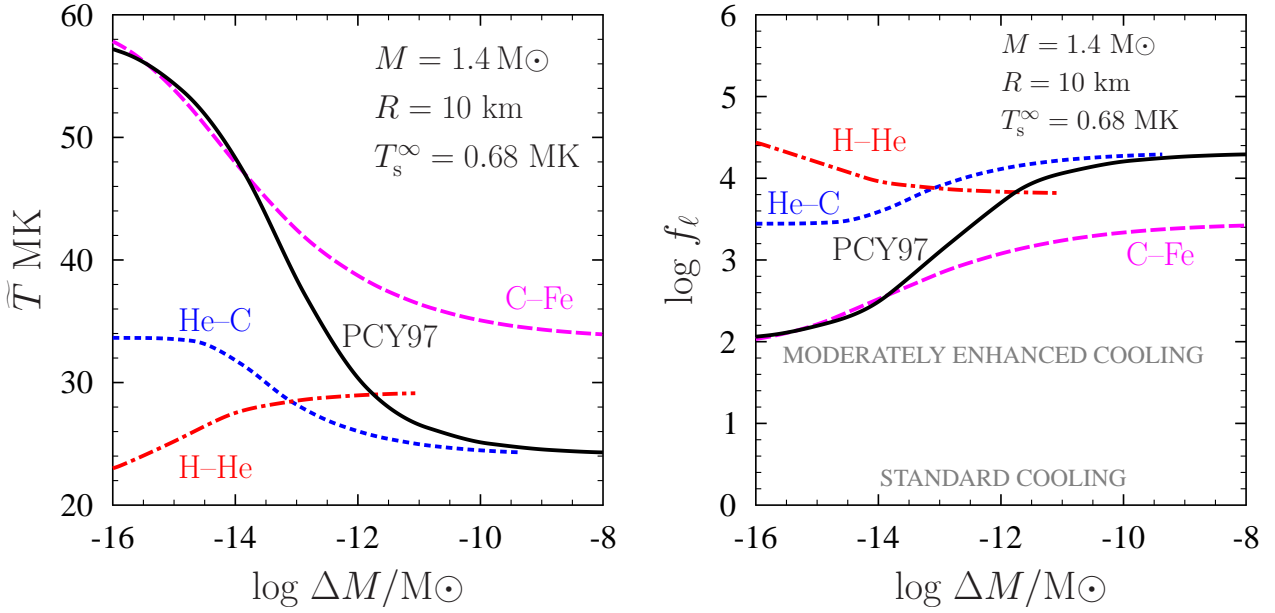


Figure 1. Internal temperature \tilde{T} (left-hand panel) and neutrino cooling function f_ℓ (right-hand panel) of the Vela pulsar for H-He, He-C, and C-Fe models of heat blanketing envelopes versus mass ΔM of the lighter element in the binary mixture. For comparison, we present also \tilde{T} and f_ℓ obtained using the envelope model of Potekhin et al. (1997) (PCY97) versus the mass ΔM of accreted elements. The level of the standard neutrino cooling $f_\ell = 1$ on the right-hand panel refers to a non-superfluid star which cools via the modified Urca process. The level $f_\ell \approx 10^2$ of moderately enhanced neutrino cooling can be provided by neutrino emission due to moderately strong neutron superfluidity in the core. See text for details.

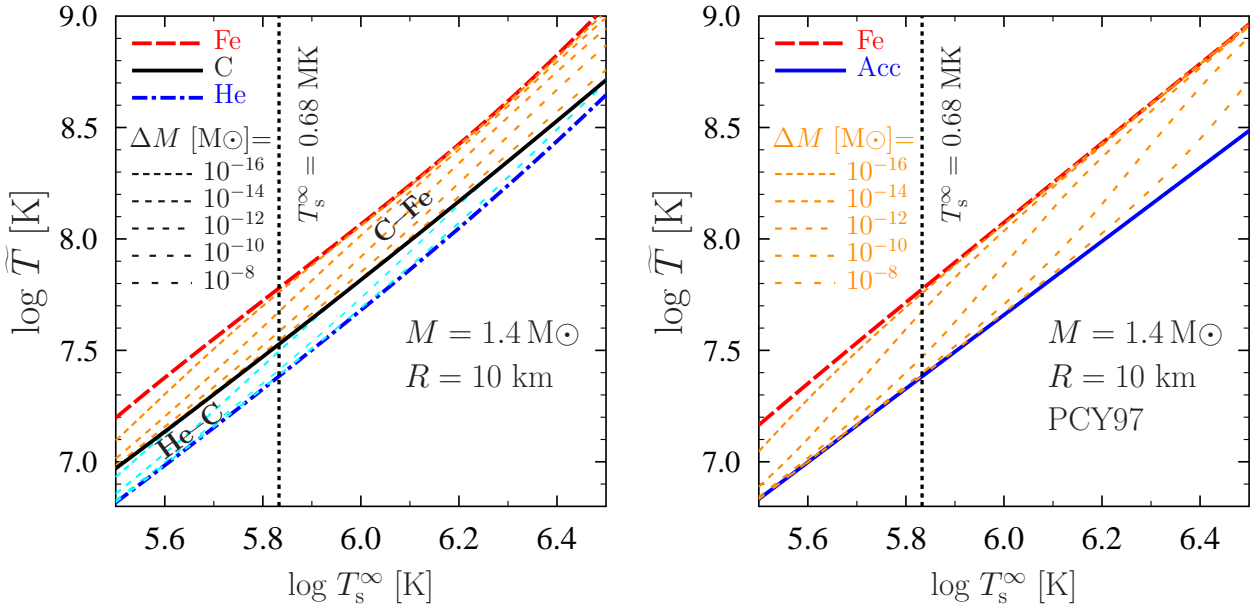


Figure 2. Thermal states (\tilde{T} versus T_s^∞) of the Vela pulsar with $M = 1.4 M_\odot$ and $R = 10$ km in the past and the future (on the right and left of the vertical dotted lines, respectively) for different chemical compositions of heat blanketing envelopes. Left-hand panel: He-C and C-Fe envelopes. The thick lines correspond from top to bottom to pure Fe, C and He envelopes, respectively. The thinner different dashed lines are for binary mixtures with different mass ΔM of lighter elements. Right-hand panel: the PCY97 envelope. The thick lines are for pure Fe and pure accreted matter; the thinner dashed lines are for different mass of the accreted matter. For given envelope models at a fixed T_s^∞ the internal temperature \tilde{T} increases when ΔM decreases.

3 THERMAL STATE OF THE VELA PULSAR

Having a theoretical $T_s - T_b$ relation and the values of T_s inferred from observations one can calculate the internal temperature of a neutron star.

Let us illustrate this by taking the Vela pulsar as an example. It is a middle-aged pulsar (with the characteristic pulsar age ≈ 11 kyr). Its internal thermal relaxation occurred long ago, so that its redshifted internal temperature \tilde{T} is constant over the pulsar interior (excluding the heat blanketing envelope). Using the magnetic hydrogen atmosphere model and taking a gravitational mass $M = 1.4 M_\odot$ and a circumferential radius of the star $R = 10$ km [with an apparent radius $R^\infty = R/\sqrt{1-x_g} = 13$ km, where $x_g = 2GM/(Rc^2)$] Pavlov et al. (2001) inferred the redshifted effective surface temperature $T_s^\infty = 0.68 \pm 0.03$ MK (at 68 per cent confidence level). To be specific, we employ $T_s^\infty = 0.68$ MK which corresponds to $T_s = T_s^\infty/\sqrt{1-x_g} = 0.888$ MK. Using a $T_s - T_b$ relation we can immediately calculate T_b and the redshifted internal temperature $\tilde{T} = T_b\sqrt{1-x_g}$. Note that the Vela pulsar possesses a magnetic field $B \sim 3 \times 10^{12}$ G, while we, following Beznogov et al. (2016), neglect the effects of magnetic fields on the heat blanketing envelope (as already mentioned above). We do it for simplicity and illustration. In addition, such magnetic fields do not affect strongly the $T_s - T_b$ relations (Potekhin et al. 2003).

The left-hand panel of Fig. 1 shows the inferred internal Vela's temperature \tilde{T} determined for a number of envelope models. The short-dashed line corresponds to \tilde{T} for the He-C envelope with $\rho_b = 10^{10}$ g cm $^{-3}$ as a function of $\Delta M = \Delta M_{\text{He}}$. The long-dashed line is the same for the C-Fe envelope versus mass of carbon, $\Delta M = \Delta M_C$. The dot-dashed line is for the H-He envelope with $\rho_b = 10^8$ g cm $^{-3}$ (at higher ρ_b He starts to burn in pycno-nuclear reactions) versus mass of hydrogen, $\Delta M = \Delta M_H$. The line is extended only to $\Delta M_H \sim 10^{-11} M_\odot$ to which hydrogen can survive in dense matter (e.g. Section 1). Finally, the solid PCY97 curve shows \tilde{T} for the H-He-C-Fe envelope of Potekhin et al. (1997) versus the mass ΔM of 'accreted' elements (H+He+C). The line for the H-He envelope is plotted up to $\Delta M \sim 10^{-11} M_\odot$, for the He-C envelope – up to $\Delta M \sim 10^{-9} M_\odot$, two other lines are plotted up to $\Delta M = 10^{-8} M_\odot$, an approximate value of ΔM to which corresponding envelopes can survive; see Section 1.

For larger ΔM we have a more heat transparent envelope with smaller internal temperature \tilde{T} for the same surface temperature T_s^∞ . An exception from this rule is provided by the H-He envelope where the situation is inverted as explained by Beznogov et al. (2016). One can see that the variations of \tilde{T} with ΔM , indeed, prevent the accurate determination of \tilde{T} if the envelope composition is unknown. The strongest variations are seen to occur for the PCY97 model, which takes into account a wider range of elements. In the case of binary mixtures, the variations become smaller, and they are especially small for the H-He and He-C mixtures.

Since the Vela pulsar is at the neutrino cooling stage with an isothermal interior, its internal temperature \tilde{T} determines (e.g., Yakovlev et al. 2011; Weisskopf et al. 2011) the fundamental parameter of superdense matter in its core, which is the neutrino cooling function

$$\ell(\tilde{T}) = L_\nu^\infty(\tilde{T})/C(\tilde{T}), \quad (1)$$

where L_ν^∞ is the redshifted neutrino luminosity of the star, and C is its heat capacity; both quantities are mainly determined by the star's core. The convenient unit of $\ell(\tilde{T}) = \ell(\tilde{T})_{\text{SC}} \propto \tilde{T}^7$ is provided by the so-called standard neutrino candle. It corresponds to a non-superfluid star which cools via the modified Urca processes of neutrino emission. Yakovlev et al. (2011) as well as Ofengeim et al. (2015) obtained analytic approximations for $\ell(\tilde{T})_{\text{SC}}$ calculated for a number of neutron star models with different masses and nucleonic equations of state (EOSs) in the core. These approximations are universal (almost independent of the EOS) and more or less equivalent (Ofengeim et al. 2015). They permit a model-independent analysis of the thermal states of neutron stars. Such an analysis has been performed previously for the Crab pulsar (Weisskopf et al. 2011); for the neutron star in the Cas A supernova remnant neglecting and including its possible rapid cooling in the present epoch (Yakovlev et al. 2011; Shternin & Yakovlev 2015); and for the neutron star in the HESS J1731-347 supernova remnant (Ofengeim et al. 2015).

Let us perform similar analysis for the Vela pulsar. Taking possible values of \tilde{T} from the right-hand panel of Fig. 1 we can reconstruct $\ell(\tilde{T})$. Using the theoretical relations derived by Yakovlev et al. (2011) or Ofengeim et al. (2015) we assume that the neutrino cooling function of the Vela pulsar behaves as $\ell(\tilde{T}) \propto \tilde{T}^7$. Then we can determine $\ell(\tilde{T})$ for any value of \tilde{T} and find

$$f_\ell = \ell(\tilde{T})/\ell(\tilde{T})_{\text{SC}}, \quad (2)$$

which is the Vela's neutrino cooling function expressed in terms of standard candles. This analysis is valid for a wide range of physical scenarios including (i) the standard candle cooling, $f_\ell = 1$; (ii) slower cooling through nucleon-nucleon bremsstrahlung of neutrino pairs if the modified Urca process is suppressed by strong neutron or proton superfluidity ($0.01 \lesssim f_\ell < 1$); (iii) faster cooling via neutrino emission due to moderately strong triplet-state Cooper pairing of neutrons in the core ($1 < f_\ell \lesssim 10^2$).

It is well known that the Vela pulsar cools somewhat faster than the standard candle (e.g., Page et al. 2004; Yakovlev & Pethick 2004) so that $f_\ell > 1$. The values of f_ℓ derived from the values of \tilde{T} are plotted on the right-hand panel of Fig. 1 as a function of ΔM . In order to infer f_ℓ we have used theoretical formulae from Ofengeim et al. (2015), but the formulae from Yakovlev et al. (2011) would give similar results. As on the left-hand panel, the lines of different types refer to the different models of heat insulation in the Vela's envelope. The dependence of f_ℓ on the chemical composition of the envelope is seen to be very strong. By increasing the mass of accreted matter in the PCY97 model to the maximum possible value $\Delta M \sim 10^{-8} M_\odot$ we increase f_ℓ from about 10^2 to 2×10^4 . Similarly, increasing the mass of carbon in the C-Fe envelope we vary f_ℓ from about 10^2 to 2.5×10^3 . Finally, by increasing the mass of He in the He-C envelope or the mass of H in the H-He envelope we can vary f_ℓ within about one decade around $f_\ell \sim 10^4$.

These results indicate once more that the chemical composition of the envelope is of great importance for studying the internal structure of neutron stars. In addition, the results for the Vela pulsar allow us to draw an important conclusion. Specifically, let us assume that we wish to describe the cooling of isolated neutron stars using the minimal cool-

ing theory (Page et al. 2004; Gusakov et al. 2004). In this theory, neutron stars have a nucleon core, the powerful direct Urca process of neutrino emission (Lattimer et al. 1991) is forbidden, and the cooling enhancement over the standard neutrino candle is provided by the neutrino emission due to a moderately strong triplet-state Cooper pairing of neutrons. The minimal cooling theory states that in this case the enhancement is limited to $f_\ell \lesssim 10^2$. Within the minimum cooling paradigm, according to the right-hand panel of Fig. 1, the Vela pulsar cannot possess H–He or He–C envelopes. Its envelope should be mostly composed of iron. Its core should mainly contain moderately strong neutron superfluidity to ensure the maximum neutrino emission enhancement $f_\ell \sim 10^2$. The Vela pulsar is the isolated neutron star coldest for its age. Its cooling regime should be similar to that of the Cas A neutron star if the current rapid cooling of the Cas A star is real (Heinke & Ho 2010; Page et al. 2011; Shternin et al. 2011; Elshamouty et al. 2013; see, however, Posselt et al. 2013 for the alternative view on the rapid cooling of the Cas A star). The Cas A neutron star is just younger but could become as cold as Vela in about 10 kyr.

On the other hand, we can adopt another cooling theory which would allow for the existence of stronger neutrino emission (e.g., Yakovlev & Pethick 2004) in the Vela pulsar, for instance, due to direct Urca process or due to similar processes enhanced, for instance, by pion condensation. Then the composition of the envelope would become again rather uncertain which would strongly complicate theoretical analysis of the internal structure of the Vela pulsar.

In Fig. 2 we show thermal states of the Vela pulsar in the past and the future for the same assumptions of $M = 1.4 M_\odot$ and $R = 10$ km as in Pavlov et al. (2001) and for different models of the envelopes from Fig. 1. The thermal states are characterized by the values of \tilde{T} versus T_s^∞ . The vertical dotted lines refer to the present epoch ($t = 11$ kr, $T_s^\infty = 0.68$ MK). The left-hand panel corresponds to the C–Fe and He–C envelopes. The thick lines are for the envelopes of pure elements: Fe (long-dashed line), C (solid line), and He (dash-dotted line). The thin dashed lines with different dash separations refer to binary mixtures with different masses of lighter elements, $\Delta M/M_\odot = 10^{-16}$, 10^{-14} , 10^{-12} , 10^{-10} and 10^{-8} . The lowest ΔM corresponds to a very thin outer layer of lighter element while the largest ΔM to the envelopes with a very thin bottom layer of heavier element. One can observe the evolution of $\tilde{T}(T_s^\infty)$ with increasing ΔM from the $\tilde{T}(T_s^\infty)$ dependence for pure heavier to pure lighter element. The older the star (the smaller T_s^∞) the smaller mass of lighter element affects \tilde{T} .

The right-hand panel of Fig. 2 shows the thermal states of the Vela pulsar for the PCY97 envelopes. The upper thick line is again for pure Fe while the lower line is for purely accreted matter. The thin lines refer to different masses of accreted matter. Note that the normalized neutrino cooling function f_ℓ (in units of standard candles) does not evolve in time as long as $\ell(\tilde{T}) \propto \tilde{T}^7$ but remains the same as plotted on the right-hand panel of Fig. 1.

4 EXAMPLES OF COOLING CALCULATIONS

Detailed calculations of neutron star cooling with new envelope models are outside the scope of this paper. Let us outline some selected results.

To be specific, we restrict ourselves to the minimal cooling paradigm (Page et al. 2004; Gusakov et al. 2004) mentioned above. Then the main regulators of neutron star cooling are (i) the neutrino emission level, f_ℓ (which can vary from $\sim 10^{-2}$ to $\sim 10^2$ depending on superfluidity of neutrons and protons in the core) and (ii) the composition of the envelope. Fixing f_ℓ and the envelope model but varying ΔM , we obtain a sequence of the cooling curves $T_s^\infty(t)$. As a rule these curves are almost ‘universal’, independent of the EOS in the core and of the star’s mass M . This is demonstrated, for instance, in figs. 24–26 of Yakovlev et al. (2001) for the case of standard neutrino candles ($f_\ell = 1$, no superfluidity) and iron envelopes.

For illustration, let us assume $f_\ell = 1$ and focus on the effect of the envelopes. Let us choose one neutron star model of mass $M = 1.4 M_\odot$ with the BSk21 EOS (Goriely et al. 2010; Pearson et al. 2012; Potekhin et al. 2013). The stellar radius will then be $R = 12.60$ km, and the direct Urca process of neutrino emission will be forbidden. The four panels of Fig. 3 show bands of the cooling curves for such a star having different envelopes (from left to right: H–He, He–C, C–Fe, and PCY97, respectively). Computations have been done using our general relativistic cooling code (Gnedin et al. 2001) and cross checked with the ‘NScool’ cooling code by D. Page¹. The results of comparison are satisfactory: calculated cooling curves differ slightly only at $t \gtrsim 2$ Myr. The initial segments of the cooling curves, $t \lesssim 10^2$ yrs refer to the initial thermal relaxation within the star (e.g., Yakovlev & Pethick 2004).

A band on each panel of Fig. 3 is restricted by upper and lower cooling curves (corresponding to almost pure He and H; He and C; C and Fe; acc and Fe, respectively; ‘acc’ refers to a fully accreted PCY97 envelope). Short-dashed lines show some intermediate cooling curves for a few values of ΔM to demonstrate that the bands are actually filled by cooling curves with different ΔM . Note that different binary mixtures are considered at different ρ_b (the same as used in Section 3). Accordingly the He cooling curve for the H–He envelope is somewhat different from the He curve for the He–C envelope.

Varying ΔM for the same envelope model, we change $T_s^\infty(t)$. This can be treated as the ‘broadening’ of the cooling curve (because, as a rule, ΔM is unknown). As seen from Fig. 3, for the H–He and He–C envelopes this broadening seems weak. However, for the C–Fe and PCY97 envelopes (where the properties of various ion species, particularly, their thermal insulation differ stronger) the broadening is large and prevents the determination of the internal temperature \tilde{T} from observations.

¹ ‘NScool’ cooling code is available at <http://www.astroscu.unam.mx/neutrones/NSCool/>.

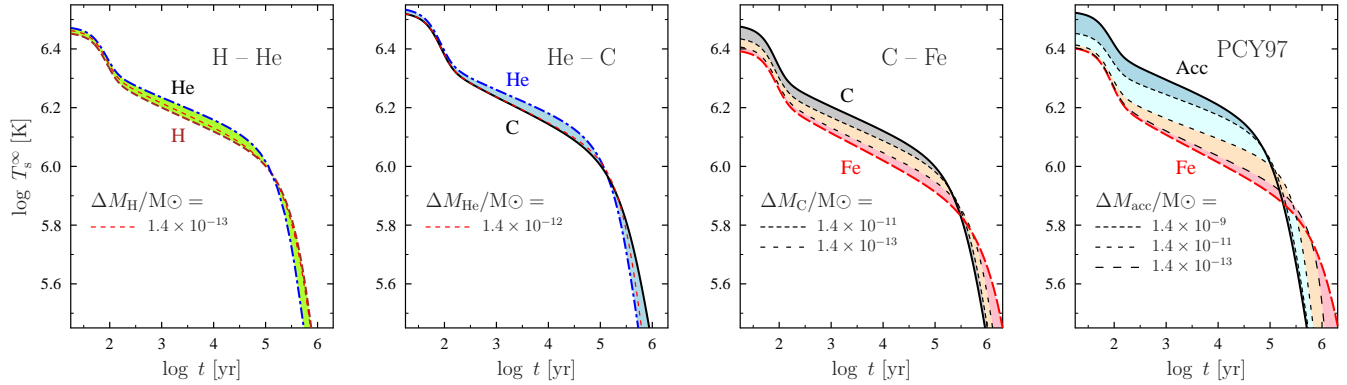


Figure 3. Cooling curves (redshifted effective surface temperature T_s^∞ versus age t) for a $1.4 M_\odot$ non-superfluid neutron star with the BSk21 EOS, different chemical compositions of heat blanketing envelopes (from left to right: H–He, He–C, C–Fe, PCY97) and different accumulated masses of lighter elements. The curves for the envelopes with maximum ΔM , containing almost entirely lighter elements, correspond (from left to right) to $\Delta M_H \sim 10^{-11} M_\odot$, $\Delta M_{He} \sim 10^{-9} M_\odot$, $\Delta M_C \sim 10^{-7} M_\odot$ and $\Delta M_{acc} \sim 10^{-7} M_\odot$, respectively. The curves for the envelopes with virtually no lighter elements are calculated for $\Delta M \sim 10^{-18} M_\odot$. See text for details.

5 PHOTON COOLING STAGE

Another important feature of the cooling curves for different ΔM in Fig. 3 is their inversion at certain t when the band of the curves becomes thin and then wider again. The inversion is accompanied by the interchange of the cooling curves. For instance, before the inversion on the right-hand panel the lowest cooling curve is for the iron envelope while after the inversion the iron envelope produces the highest cooling curve. The inversion epoch changes from $t \approx 10^5$ yr for the lighter H–He and He–C envelopes to $(2-3) \times 10^5$ yr for the heavier C–Fe and PCY97 envelopes.

These inversions are well known in the literature (e.g. Yakovlev & Pethick 2004). They manifest the transition from the neutrino cooling stage to the photon cooling stage. The transition period is relatively short. The transition has a dramatic impact on the cooling process. At the neutrino cooling stage, a star cools via neutrinos from the interior and looks colder for a more insulating envelope composed of heavier elements. At the photon cooling stage, the star cools via photons from the surface. The neutrino emission becomes insignificant for the cooling process, and the cooling is governed by the heat capacity of the core and the heat transparency of the envelope. More insulating envelopes of heavier elements produce hotter stars.

Fig. 4 shows a selection of theoretical cooling curves from Fig. 3 that are obtained for a $1.4 M_\odot$ nonsuperfluid star with the BSk21 EOS in the core. The four thick curves correspond to the envelopes made of pure Fe (the long-dashed line), C (the solid line), He (the dot-dashed line) and of pure accreted matter in the envelope model of PCY97 (the short-dashed line). The space between the Fe and C curves is filled by the cooling curves for the C–Fe envelope with different ΔM . The space between the C and He curves is filled by the cooling curves for the He–C envelope. The space between the Fe and acc curves is covered by the cooling curves for the PCY97 envelope. To simplify Fig. 4 we do not present the results for the H–He envelope which can be easily visualized from the left-hand panel of Fig. 3.

In addition, Fig. 4 presents the observational data on the isolated middle-aged neutron stars. The data are the

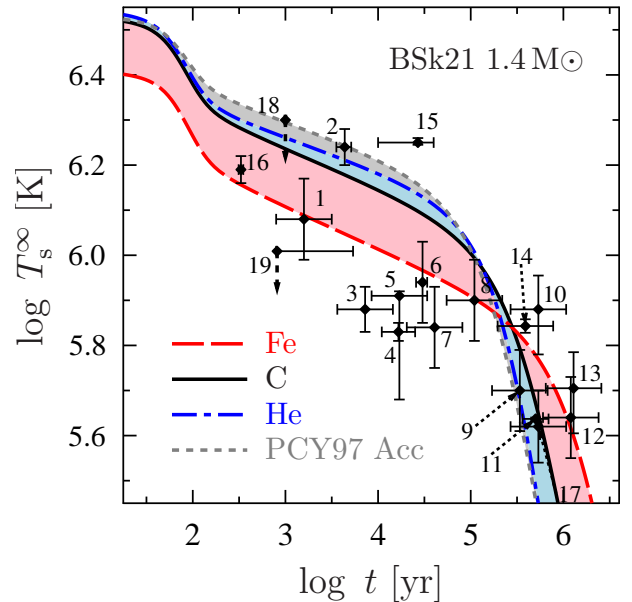


Figure 4. Cooling curves for a $1.4 M_\odot$ non-superfluid (standard neutrino candle) neutron star with the BSk21 EOS. The thick lines correspond to envelopes of pure Fe, C, He, as well as of pure accreted matter in the PCY97 model. The filled area between the Fe and C curves is covered by cooling curves for C–Fe envelopes with different ΔM ; similarly, the space between the C and He curves can be covered with cooling curves for He–C envelopes. The area between the Fe and acc curves is covered by cooling curves for the PCY97 envelope. The cooling curves are compared with the observations of isolated neutron stars. See the text for details.

same as those presented in Beznogov & Yakovlev (2015a,b); Ofengeim et al. (2015); references to original publications can also be found there. Neutron star labels are as follows, (1) PSR J1119–6127; (2) RX J0822–4300 (in Pup A); (3) PSR J1357–6429; (4) PSR B0833–45 (Vela); (5) PSR B1706–44; (6) PSR J0538+2817; (7) PSR B2334+61; (8) PSR B0656+14; (9) PSR B0633+1748 (Geminga); (10) PSR B1055–52; (11) RX J1856.4–3754; (12) PSR J2043+2740;

(13) RX J0720.4–3125; (14) PSR J1741–2054; (15) XMMU J1732–3445; (16) Cas A neutron star; (17) PSR J0357+3205 (Morla); (18) PSR B0531+21 (Crab); (19) PSR J0205+6449 (in 3C 58).

First let us outline briefly the sources which are at the neutrino cooling stage ($t \lesssim 10^5$ yr). Recall that for a standard neutrino candle with an iron envelope we would have one Fe (thick long-dashed) cooling curve which cannot explain many data. As seen from Fig. 4, even varying the composition of the envelope of the standard candle we can explain much more sources, although not all of them. The explanation of other sources at the neutrino cooling stage would require deviations from the standard neutrino candle (from $f_\ell = 1$). For instance, the hottest XMMU J1732–3445 source can be explained assuming nearly maximum amount of carbon in the envelope and strong proton superfluidity in the core ($f_\ell \sim 0.01$, Klochkov et al. 2015; Ofengeim et al. 2015). The coldest sources at the neutrino cooling stage, like the Vela pulsar, can be interpreted, for instance, as neutron stars with moderately strong triplet-state neutron pairing in the core which increases the neutrino cooling level to $f_\ell \sim 10^2$ (Section 3).

Now let us focus on the sources at the photon cooling stage (after the inversion of the cooling curves). It is not a surprise (Fig. 4) that all these sources are compatible with the standard neutrino cooling candle (see below). The variety of such sources can be explained by different composition of their envelopes. The hottest neutron stars at the photon cooling stage (like PSR B1055–52, Pavlov & Zavlin 2003; PSR J2043+2740, Zavlin 2009; RX J0720.4–3125, Motch et al. 2003) should have their envelope made predominantly of iron while the coldest stars (like Geminga, Kargaltsev et al. 2005; RX J1856.4–3754, Ho et al. 2007; Potekhin 2014) may have envelopes of lighter elements (for instance, carbon).

Note that although the evolution of neutron stars at the photon cooling stage does not depend directly on their neutrino emission, the observed sources with $t \gtrsim 10^5$ yr should not have $f_\ell \gg 1$. Otherwise they would cool rapidly at the neutrino cooling stage, transit to the photon cooling stage earlier and would become very weak at $t \gtrsim 10^5$ yrs. Therefore, the hottest neutron stars at the photon cooling stage seem to be those which have $f_\ell \lesssim 1$ and possess Fe envelopes (which are better thermal insulators than the envelopes of lighter elements).

The effects of heat blanketing envelopes on the cooling of the neutron stars with different masses, radii, equations of state of superdense matter, magnetic fields, and superfluid properties have been extensively studied using the PCY97 envelopes and their magnetic extensions (see, e.g., Yakovlev & Pethick 2004; Kaminker et al. 2006; Potekhin et al. 2015; Beznogov & Yakovlev 2015a and references therein). For instance, it is well known that all cooling curves $T_s^\infty(t)$ for non-superfluid neutron stars of different masses which cool via modified Urca process ($f_\ell = 1$) and have iron heat blanketing envelopes but no strong magnetic fields, merge in almost one and the same cooling curve. The same is also true for the stars with fully accreted PCY97 heat blanketing envelopes although the curve becomes different. We have checked that this property survives for the new envelope models of Beznogov et al. (2016).

The above analysis has neglected possible mechanisms

of neutron star reheating, for instance, due to ohmic decay of magnetic fields, possible violations of beta-equilibrium, etc.; e.g., Yakovlev & Pethick (2004); Page et al. (2006) and references therein. Were these mechanisms operative they would be able to keep neutron stars warmer. No such mechanisms seem to be required for ordinary cooling middle-aged neutron stars.

6 CONCLUSIONS

We have outlined the effects of our new models for heat blanketing envelopes (Beznogov et al. 2016) of neutron stars on the cooling and thermal structure of isolated middle-aged neutron stars. The new envelopes are composed of binary ionic mixtures (either H–He, or He–C, or C–Fe) with any allowed mass ΔM of lighter elements. The results are compared with the standard PCY97 models of the envelopes containing shells of H, He, C, and Fe with any possible mass of ‘accreted’ (H+He+C) elements (Potekhin et al. 1997). As discussed in Beznogov et al. (2016), the new models allow one to consider wider classes of the envelopes.

In Section 2 we have outlined some formation scenarios of the envelopes. In Section 3 we have considered the effects of the envelopes on inferring the internal temperatures \tilde{T} of neutron stars from observations and on constraining their neutrino cooling function f_ℓ (the fundamental parameter of superdense matter in a neutron star core). We have taken the Vela pulsar as an example. The results confirm previous conclusions (e.g., Yakovlev et al. 2011; Weisskopf et al. 2011; Klochkov et al. 2015; Ofengeim et al. 2015) that the composition of the heat blanketing envelope is a major ingredient for the correct interpretation of observations. The uncertainty in the envelope composition translates into a factor of $\sim 10^2$ uncertainty in f_ℓ . Nevertheless, since the Vela pulsar is sufficiently cold (Pavlov et al. 2001), we have been able to conclude that within the minimal cooling scenario the pulsar should have $f_\ell \sim 10^2$ and the envelope predominantly made of iron.

In Sections 4 and 5 we have performed some cooling calculations for a $1.4 M_\odot$ neutron star with different envelopes and compared the results with observations. A special emphasis has been made on neutron stars of ages $t \sim 0.1$ – 1 Myr which have changed their cooling regime from the earlier neutrino cooling to the photon cooling. We have shown that all observations of such stars (including PSR B1055–52, PSR J2043+2740, RX J0720.4–3125, Geminga, and RX J1856.4–3754) are consistent with the scenario in which these stars were initially nearly standard neutrino candles or slower neutrino coolers ($f_\ell \lesssim 1$) but possess various envelopes mostly containing carbon and iron.

Our consideration is definitely not complete. More work is required to overcome the problem of heat blanketing envelopes in the theory of thermal evolution of neutron stars. In particular, more complicated models of the envelopes can be constructed taking into account multicomponent ion mixtures in and out of diffusive equilibrium; the dynamical evolution of the diffusive equilibrium can also be modelled. In addition, one can elaborate the existing models of diffusive nuclear burning in the envelopes (e.g., Chang & Bildsten 2003, 2004; Chang et al. 2010) which is neglected here. It would also be very important to include the effects of mag-

netic fields (Potekhin et al. 2015) on the envelopes of various types. Any additional reliable information on the formation history and evolution of the envelopes would also be most welcome. However, all these problems go far beyond the scope of the present investigation.

ACKNOWLEDGEMENTS

The work of MB was partly supported by the Dynasty Foundation, the work of DG by the Russian Foundation for Basic Research (grants 14-02-00868-a and 16-29-13009-ofi-m), and the work of MF, PH, and LZ was supported by the Polish NCN research grant no. 2013/11/B/ST9/04528.

REFERENCES

- Beznogov M. V., Yakovlev D. G., 2015a, *MNRAS*, **447**, 1598
 Beznogov M. V., Yakovlev D. G., 2015b, *MNRAS*, **452**, 540
 Beznogov M. V., Potekhin A. Y., Yakovlev D. G., 2016, *MNRAS*, **459**, 1569
 Blaes O. M., Blandford R. D., Madau P., Yan L., 1992, *ApJ*, **399**, 634
 Brown E. F., Bildsten L., Chang P., 2002, *ApJ*, **574**, 920
 Chang P., Bildsten L., 2003, *ApJ*, **585**, 464
 Chang P., Bildsten L., 2004, *ApJ*, **605**, 830
 Chang P., Bildsten L., Arras P., 2010, *ApJ*, **723**, 719
 Elshamouty K. G., Heinke C. O., Sivakoff G. R., Ho W. C. G., Shternin P. S., Yakovlev D. G., Patnaude D. J., David L., 2013, *ApJ*, **777**, 22
 Gnedin O. Y., Yakovlev D. G., Potekhin A. Y., 2001, *MNRAS*, **324**, 725
 Goriely S., Chamel N., Pearson J. M., 2010, *Phys. Rev. C*, **82**, 035804
 Gusakov M. E., Kaminker A. D., Yakovlev D. G., Gnedin O. Y., 2004, *A&A*, **423**, 1063
 Heinke C. O., Ho W. C. G., 2010, *ApJL*, **719**, L167
 Ho W. C. G., Heinke C. O., 2009, *Nature*, **462**, 71
 Ho W. C. G., Kaplan D. L., Chang P., van Adelsberg M., Potekhin A. Y., 2007, *MNRAS*, **375**, 821
 Kaminker A. D., Gusakov M. E., Yakovlev D. G., Gnedin O. Y., 2006, *MNRAS*, **365**, 1300
 Kargaltsev O. Y., Pavlov G. G., Zavlin V. E., Romani R. W., 2005, *ApJ*, **625**, 307
 Klochkov D., Pühlhofer G., Suleimanov V., Simon S., Werner K., Santangelo A., 2013, *A&A*, **556**, A41
 Klochkov D., Suleimanov V., Pühlhofer G., Yakovlev D. G., Santangelo A., Werner K., 2015, *A&A*, **573**, A53
 Lattimer J. M., Pethick C. J., Prakash M., Haensel P., 1991, *Phys. Rev. Lett.*, **66**, 2701
 Lattimer J. M., van Riper K. A., Prakash M., Prakash M., 1994, *ApJ*, **425**, 802
 Motch C., Zavlin V. E., Haberl F., 2003, *A&A*, **408**, 323
 Ofengeim D. D., Kaminker A. D., Klochkov D., Suleimanov V., Yakovlev D. G., 2015, *MNRAS*, **454**, 2668
 Page D., Lattimer J. M., Prakash M., Steiner A. W., 2004, *ApJS*, **155**, 623
 Page D., Geppert U., Weber F., 2006, *Nucl. Phys. A*, **777**, 497
 Page D., Lattimer J. M., Prakash M., Steiner A. W., 2009, *ApJ*, **707**, 1131
 Page D., Prakash M., Lattimer J. M., Steiner A. W., 2011, *Phys. Rev. Lett.*, **106**, 081101
 Pavlov G. G., Zavlin V. E., 2003, in Bandiera R., Maiolino R., Mannucci F., eds, *Texas in Tuscany. XXI Symposium on Relativistic Astrophysics*. pp 319–328
 Pavlov G. G., Zavlin V. E., Sanwal D., Burwitz V., Garmire G. P., 2001, *ApJL*, **552**, L129
 Pearson J. M., Chamel N., Goriely S., Ducoin C., 2012, *Phys. Rev. C*, **85**, 065803
 Posselt B., Pavlov G. G., Suleimanov V., Kargaltsev O., 2013, *ApJ*, **779**, 186
 Potekhin A. Y., 2014, *Phys.-Usp.*, **57**, 735
 Potekhin A. Y., Chabrier G., Yakovlev D. G., 1997, *A&A*, **323**, 415
 Potekhin A. Y., Yakovlev D. G., Chabrier G., Gnedin O. Y., 2003, *ApJ*, **594**, 404
 Potekhin A. Y., Fantina A. F., Chamel N., Pearson J. M., Goriely S., 2013, *A&A*, **560**, A48
 Potekhin A. Y., Pons J. A., Page D., 2015, *Space Sci. Rev.*, **191**, 239
 Rosen L. C., 1968, *Ap&SS*, **1**, 372
 Shternin P. S., Yakovlev D. G., 2015, *MNRAS*, **446**, 3621
 Shternin P. S., Yakovlev D. G., Heinke C. O., Ho W. C. G., Patnaude D. J., 2011, *MNRAS*, **412**, L108
 Weisskopf M. C., Tennant A. F., Yakovlev D. G., Harding A., Zavlin V. E., O’Dell S. L., Elsner R. F., Becker W., 2011, *ApJ*, **743**, 139
 Yakovlev D. G., Pethick C. J., 2004, *ARA&A*, **42**, 169
 Yakovlev D. G., Kaminker A. D., Gnedin O. Y., Haensel P., 2001, *Phys. Rep.*, **354**, 1
 Yakovlev D. G., Ho W. C. G., Shternin P. S., Heinke C. O., Potekhin A. Y., 2011, *MNRAS*, **411**, 1977
 Zavlin V. E., 2009, in Becker W., ed., *Astrophysics and Space Science Library Vol. 357, Neutron Stars and Pulsars*. p. 181

This paper has been typeset from a $\text{\TeX}/\text{\LaTeX}$ file prepared by the author.